



**HAL**  
open science

# Multichannel Multiple Signal Classification for dispersion curves extraction of ultrasonic guided waves

Paul Zabbal, Guillemette Ribay, Bastien Chapuis, Julien Jumel

## ► To cite this version:

Paul Zabbal, Guillemette Ribay, Bastien Chapuis, Julien Jumel. Multichannel Multiple Signal Classification for dispersion curves extraction of ultrasonic guided waves. *Journal of the Acoustical Society of America*, 2018, 143, pp.EL87 - EL92. 10.1121/1.5022699 . cea-01765665

**HAL Id: cea-01765665**

**<https://cea.hal.science/cea-01765665>**

Submitted on 10 Jan 2019

**HAL** is a multi-disciplinary open access archive for the deposit and dissemination of scientific research documents, whether they are published or not. The documents may come from teaching and research institutions in France or abroad, or from public or private research centers.

L'archive ouverte pluridisciplinaire **HAL**, est destinée au dépôt et à la diffusion de documents scientifiques de niveau recherche, publiés ou non, émanant des établissements d'enseignement et de recherche français ou étrangers, des laboratoires publics ou privés.

# Multichannel Multiple Signal Classification for dispersion curves extraction of ultrasonic guided waves

Paul Zabbal,<sup>1,a)</sup> Guillemette Ribay,<sup>1</sup> Bastien Chapuis,<sup>1</sup>  
and Julien Jumel<sup>2</sup>

<sup>1</sup>CEA (The French Atomic Energy Commission), LIST (Laboratory for Integration of Systems and Technology), Gif-sur-Yvette F-91191, France

<sup>2</sup>University of Bordeaux, CNRS, Arts et Metiers ParisTech, I2M, UMR 5295, F-33400 Talence, France

paul.zabbal@cea.fr, guillemette.ribay@cea.fr, bastien.chapuis@cea.fr,  
julien.jumel@u-bordeaux.fr

**Abstract:** Multichannel acquisition of ultrasonic guided waves can be used to extract dispersion curves, from the time-position domain ( $t-x$ ) to the frequency-wavenumber ( $f-k$ ), or frequency-velocity domain ( $f-c$ ). Accurate measurements are needed in order to be able to precisely characterize the specimen, by improving the extraction of low amplitude modes and enhance resolution. The proposed method is based on the Multiple Signal Classification algorithm combined with a multi-emitter and multi-receiver acquisition. In this work, this method is applied on experimental data to extract dispersive information from multilayered bonded specimens.

## 1. Introduction

Ultrasonic guided waves have been used in many industrial applications in nondestructive testing, from material characterization to structural health monitoring. Guided waves are dispersive, directly dependent on the frequency, thickness, and material properties. Therefore the dispersion curves contain a great deal of information on the tested specimen. The mapping from time-distance to frequency-wavenumber was first performed by a simple 2D-FT (two-dimensional Fourier Transform) (Alleyne and Cawley, 1991) with the use of a multichannel acquisition with a unique emitter. Dispersion extraction in ultrasonic nondestructive testing is a crucial issue and a number of methods have been developed in favor of a gain in accuracy (Xu *et al.*, 2016). Indeed, accurate measurements are needed especially in cases of high density of modes where a high resolution is needed or for low-amplitude modes in complex materials like composite. One promising method is based on the Singular Value Decomposition (SVD) applied on a multi-emitter and multi-receiver acquisition (Minonzio *et al.*, 2010) on bone testing. More recently, improvements have been made by considering this SVD method as an inverse problem (Xu *et al.*, 2016) and with a sparse regularization strategy to achieve a better extraction with the drawback of depending on heuristic parameters. Another recent use of the sparse property of the Lamb waves to reconstruct dispersion curves is performed with continuity constraints (Zhao *et al.*, 2017).

MULTiple SIGNAL Classification (MUSIC) has been applied to some specific cases for measurement of the dispersion curves. First it was used in seismic application in a passive format using several receivers (Iranpour, 2004). Then it was extended in structural health monitoring using a single emitter to extract the dispersive information (Ambrozinski *et al.*, 2015). In both cases because of the low number of sources some information can get lost. Therefore the need of optimized algorithms to retrieve the dispersion information persists.

Dispersion curves can be used to inspect adhesive bonds; however, the contributions of the interfaces or of the adhesive properties are weak and a high resolution method is needed in order to extract them (Le Crom and Castaings, 2010). We propose a method based on MUSIC combined with a multi-emitter and multi-receiver acquisition. The approach has been validated experimentally on multilayered structures with different materials such as Titane/Titane and CFRP/CFRP (carbon fiber reinforced polymer) bonds.

---

<sup>a)</sup>Author to whom correspondence should be addressed. Also at: University of Bordeaux, CNRS, Arts et Metiers ParisTech, I2M, UMR 5295, F-33400 Talence, France.

## 2. MUSIC method for dispersion extraction

This section describes both the method and the experimental setup used as a validation of the method with an example of a possible configuration.

### 2.1 Response matrix and eigendecomposition

A linear array is used in contact using coupling gel, with  $M$  emitters and  $N$  receivers, giving an inter-element response matrix of size  $M \times N$ . Our setup is similar to the one presented in Fig. 1 of Minonzio *et al.* (2010) except that the group of emitters is adjacent to the receivers. The emitted signal is denoted  $s_i$ , the received signal  $g_{ij}$ , and the impulse response between two transducers is denoted  $h_{ij}$  with  $i \in [1, M]$  and  $j \in [1, N]$ , giving us the relation Eq. (1) with  $t$  the time

$$g_{ij}(t) = h_{ij}(t) \otimes s_i(t). \quad (1)$$

If we note  $G$ ,  $H$ , and  $S$ , respectively, the FTs of  $g$ ,  $h$ , and  $s$ , the frequency impulse response is written in the form of Eq. (2),

$$G_{ij}(f) = H_{ij}(f)S_i(f). \quad (2)$$

Our method is based on the MUSIC algorithm (Schmidt, 1986) used in the frequency domain but we use it as wavenumber estimation and not spectrum estimation. The autocorrelation matrix is considered at each frequency of interest of the impulse response matrix, noted  $R_{xx}(f)$  as presented in Eq. (3), with  $E[\cdot]$  the expectation and  $^H$  denoting the Hermitian transpose of the matrix, and of size  $N \times N$ , giving the correlation coefficients between the different receivers

$$R_{xx_{ij}}(f) = E[G_{ij}G_{ij}^H]. \quad (3)$$

The autocorrelation matrix is a Hermitian matrix which can be decomposed according to the eigendecomposition:  $R_{xx}(f) = P^{-1}DP$ . The matrix  $P$  contains all the eigenvectors  $\nu$  at a specific frequency, and the diagonal matrix  $D$  contains all the eigenvalues  $\lambda$  of the matrix  $R_{xx}(f)$ . These eigenvectors can be divided into the signal and the noise sub-spaces as represented in Eq. (4), with  $p$  denoting the number of eigenvectors associated to the signals. The guided mode signals are uncorrelated to the noise and their eigenvectors are orthogonal. In this case, the number of signal eigenvectors represents the number of modes at a specific frequency propagating in the medium. The number of modes is not known *a priori* and therefore needs to be found in order to obtain the most accurate dispersion curves without loss of information. Several methods can be employed to retrieve this inflection point, from a simple threshold (Minonzio *et al.*, 2010) to Linear Regression, or even the use of a statistical model as the Akaike Information Criteria. We use the same method in each case which is based on a linear test (Williams, 1999)

$$\sum_{n=1}^N \lambda_n(f)\nu_n(f) = \sum_{n=1}^p \lambda_n(f)\nu_n(f) + \sum_{n=p+1}^N \lambda_n(f)\nu_n(f). \quad (4)$$

Subsequently, the  $N-p$  eigenvectors of the noise sub-space are used and projected on the signal subspace made of a set of  $e_k = \exp(jkx)$ , with  $x$  the vector of the distance of the receivers. The pseudospectrum is evaluated with Eq. (5) and yields the best results compared to other projectors like the Maximum Likelihood. Exploiting the orthogonal property, the pseudospectrum will have  $p$ -peaks corresponding to the  $p$ -modes at a certain frequency because the projection of the noise eigenvectors on the signal space will tend to zero. It is only a wavenumber estimation, giving the accurate positions of guided modes that were preset in the inter-element matrix but the value is not related to an energy or power of the guided wave. The relation with the energy is presented in Sec. 2.3,

$$P_{mu}(f, k) = \frac{1}{\sum_{n=p+1}^N |e_k \nu_n(f)|^2}. \quad (5)$$

### 2.2 Autocovariance matrix

The covariance matrix is directly related to the time reversal operator (Prada and Thomas, 2003). Indeed, it is equivalent to compute the eigendecomposition of the autocovariance matrix or to compute a SVD of the transfer matrix  $G^H(f)G(f)$  usually noted  $K(\omega)$  in the literature on Decomposition of the Time Reversal Operator. We can

therefore use the same MUSIC algorithm and the same projector Eq. (5) on the singular vectors of  $G^H(f)G(f)$ , which yields the same results.

### 2.3 Energy evaluation

The pseudospectrum depicts only information about the position of the dispersion curves but not the real energy on each mode, which may be useful for some nondestructive testing applications. After retrieving the exact position of each mode the energy evaluation can be computed. Indeed, by definition the eigendecomposition can be formulated as Eq. (6). The discrete energy of the guided wave modes is denoted  $E_u$  with  $u \in [1, p]$  the modes found in the previous step,  $\sigma_w$  corresponds to the noise variance and therefore is considered in first approximation as the square value of the eigenvalues associated to the noise sub-space. A new relation is found [Eq. (7)] (Hayes, 1996),

$$\forall n \in [1, P], \quad R_{xx}(f) \cdot \nu_n(f) = \lambda_n(f) \cdot \nu_n(f), \quad (6)$$

$$\sum_{u=1}^P E_u(f) \cdot |e_u^H \cdot \nu_n(f)|^2 = \lambda_n(f) - \sigma_w^2. \quad (7)$$

The energy can be retrieved by solving Eq. (8), with  $e_u = \exp(jk_u x)$ ,  $k_u$  corresponds to the wavenumber of each mode found in the wavenumber estimation step, and  $x$  is the distance vector of the receivers

$$\begin{bmatrix} |e_1^H \cdot \nu_1(f)|^2 & \cdots & |e_p^H \cdot \nu_1(f)|^2 \\ \vdots & \ddots & \vdots \\ |e_1^H \cdot \nu_p(f)|^2 & \cdots & |e_p^H \cdot \nu_p(f)|^2 \end{bmatrix} \cdot \begin{bmatrix} E_1(f) \\ \vdots \\ E_p(f) \end{bmatrix} = \begin{bmatrix} \lambda_1(f) - \sigma_w^2 \\ \vdots \\ \lambda_p(f) - \sigma_w^2 \end{bmatrix}. \quad (8)$$

### 2.4 Experimental setup

Experiments are achieved using array transducers of  $N_E$  elements associated with a specific driving electronic device, a M2M MultiX system. In this work we have, as denoted previously,  $M$  emitters and the number of receivers is  $N = N_E - M$ . The number of emitters is of great importance since it impacts the final result. Indeed, the more emitters are used the more information is present but with an increase of noise. The first temporal samples are removed before applying the algorithm because they contain signals traveling in the coupling medium that are easy to identify.

*Titane/Titane bond.* In the first case, the tested material is a 50 mm long and 50 mm wide Titane/Titane bond and the adhesive is AF 191. Each adherent has a thickness of 1.6 mm and the adhesive is 0.14 mm thick. The probe (Imasonic, Voray-sur-l'Ognon, France) consists of 128 elements, with a pitch of 0.2 mm and the length and width of each rectangular element are 0.175 and 6 mm, respectively. The central frequency is 15 MHz, with a  $-6$  dB fractional bandwidth of 60%. The number of emitters used in the MUSIC-based method is chosen to optimize qualitatively the information presented, and the number of emitters selected for the SVD-based extraction method is chosen to give the same level of information and a second picture depicting the SVD-based method with the same number of elements as with the MUSIC algorithm. The original MUSIC-based method is also used to illustrate the advantages of using multiple sources.

*Compositel/Composite bond.* The second specimen is a 200 mm long and 200 mm wide CFRP/CFRP bond with an epoxy adhesive; each adherent is 2 mm thick and

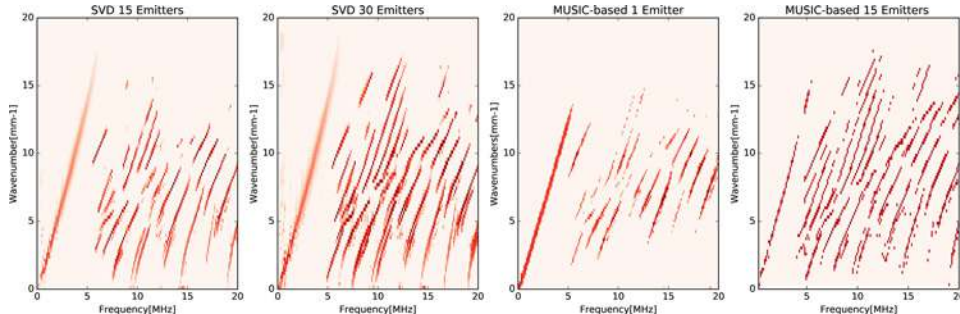


Fig. 1. (Color online) An example of comparison between the SVD-based method (15 and 30 emitters), the original MUSIC and the proposed method (15 emitters) on a Titane/Titane specimen with 1.6 mm thickness for each adherent.

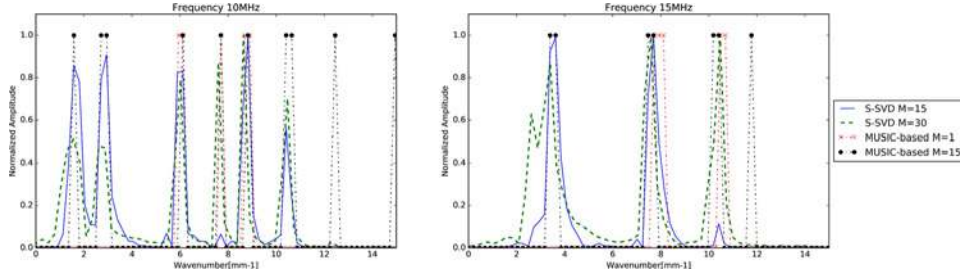


Fig. 2. (Color online) Comparison of the wavenumber resolution for the Titane/Titane bond for four different dispersion extraction methods.

the adhesive is 0.2 mm thick. The CFRP consists of 8 layers  $[0/0/45/-45/-45/45/0/0]^\circ$ . The probe (Imasonic, Voray-sur-l’Ognon, France) consists of 64 elements with a pitch of 0.8 mm, and the length and width of each rectangular element are 0.55 and 18 mm, respectively, with a center frequency of 2 MHz, with a  $-6$  dB fractional bandwidth of 60%. Again, the number of emitters is chosen to be qualitatively optimal for the MUSIC algorithm. Regarding the SVD-based method, two cases are presented: one with 20 emitters chosen to present dispersion curves similar to the MUSIC-method but with a higher noise level, and a second case with only ten emitters to reduce the noise.

### 3. Results

We compared our method with previous multichannel acquisition existing techniques to extract dispersion curves.

*Titane/Titane bond.* In this first application case we focus mainly on the ability of the MUSIC-based method to extract the dispersive curves of the guided modes, and thus not looking at the energy content at this stage. Figure 1 displays two SVD-based ( $M=15$  and  $30$ ) dispersion curve extractions (Minonzio *et al.*, 2010), the original ( $M=1$ ) and our MUSIC method ( $M=15$ ). As it can be observed, there are a high number of modes with some overlapping ones, which constitutes a perfect example where high resolution extraction is needed to distinguish the guided modes. It can be observed that in order to have qualitatively the same information present in both cases, the SVD-based method needs more emitters than with multi-channel MUSIC. The original MUSIC method exhibits a loss of information compared to the use of multiple sources.

In Fig. 2, the normalized amplitude computed at two specific frequencies are shown as a function of wavenumber using four different methods: the SVD (Minonzio *et al.*, 2010), S-SVD (Xu *et al.*, 2016), the original, and the modified MUSIC algorithm. The heuristic parameters as defined in Xu *et al.* (2016) are in this case: the 11-norm with  $\mu=0.01$ ,  $\sigma=1$ . The SVD post-processing shows noise between modes, which is corrected with the S-SVD algorithm but some modes are invisible, or at noise-level in both cases. In order to observe all present modes a high number of receivers would be needed, in detriment to noise level. Accuracy is gained with the proposed MUSIC method, and it enhances the detection of some low-amplitude modes, especially for high wavenumber.

*Composite/Composite bond.* Figure 3 displays, as previously shown, three dispersion curves with different methods: the SVD-based method either with 20 emitters or 10 emitters, and the proposed method in the case of the CFRP bond using 10

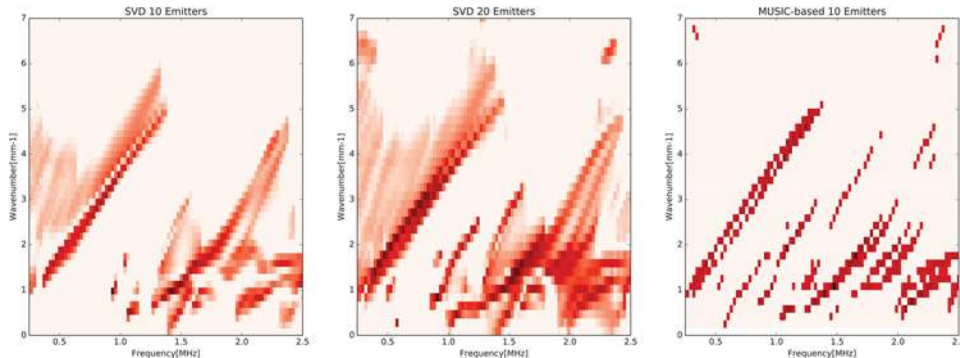


Fig. 3. (Color online) An example of comparison on a Composite/Composite specimen with 2 mm thickness for each adherent: with two cases for the SVD-based method (respectively, 10 and 20 emitters) and the proposed MUSIC algorithm (10 emitters).

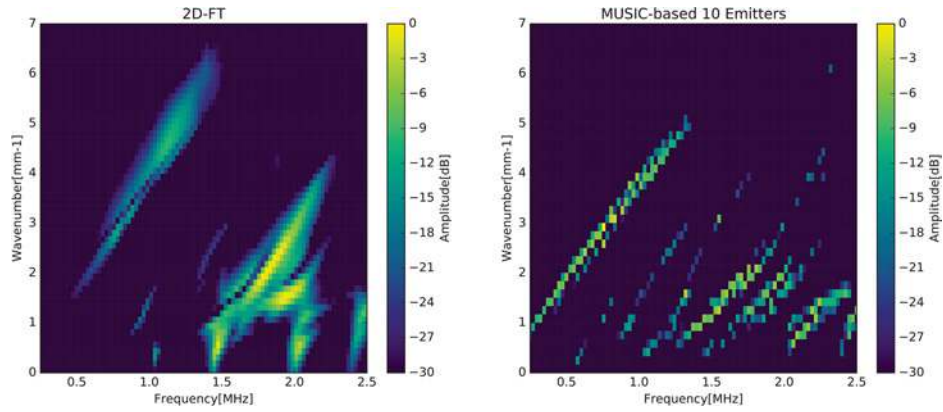


Fig. 4. (Color online) Comparison between energy calculation (in dB) with 2D-FT and MUSIC (ten emitters) applied on multiple sequences.

emitters. Dispersion curve extraction is complex for composite as it can be noisy due to higher attenuation compared to titane. The SVD-based method gains accuracy compared to the 2D-FT, which can be seen in Fig. 4, but still presents a high noise level, especially in the first case. The gain of information has a cost and a compromise has to be made.

An example of the energy evaluation is displayed in Fig. 4, where the 2D-FT and the MUSIC-based energy estimation method are compared. In the latter, even modes with very low-energy (30 dB less than the most energetic mode) are detected, whereas they are missing in the 2D-FT image.

#### 4. Conclusion

A MUSIC-based multichannel method is presented to extract dispersion curves from experimental data. It was performed on two data sets, first on the titane/titane bond with a high density of modes where a high wavenumber resolution is needed, and second on a composite/composite bond where noise is polluting the modes. Compared to the SVD-based techniques, in these cases, multichannel MUSIC enhances weak modes and displays a low noise level and a high wavenumber resolution. An automatic method to choose the number of emitters to obtain the best case scenario should be studied in the future. The present method can be used in a variety of configurations for nondestructive applications, for example, for characterization of multilayered structures of different materials. The next step is to use this method to inverse the material parameters and assess the adhesion quality of bonded joints.

#### Acknowledgments

This work was performed with support from SAFRAN which provided the different materials for the titane bonds. Part of this research was also supported by European Union's Horizon 2020 research and innovation programme under Grant Agreement No. 636494, project ComBoNDT (Quality assurance concepts for adhesive bonding of aircraft composite structures by advanced NDT), which provided the CFRP bond.

#### References and links

- Alleyne, D., and Cawley, P. (1991). "A two-dimensional Fourier transform method for the measurement of propagating multimode signals," *J. Acoust. Soc. Am.* **89**(3), 1159–1168.
- Ambrozinski, L., Packo, P., Pieczonka, L., Stepinski, T., Uhl, T., and Staszewski, W. J. (2015). "Identification of material properties—efficient modelling approach based on guided wave propagation and spatial multiple signal classification," *Struct. Control Health Monitor.* **22**(7), 969–983.
- Hayes, M. H. (1996). *Statistical Digital Signal Processing and Modeling* (John Wiley & Sons, New York), pp. 463–465.
- Iranpour, K. (2004). "Parametric fk techniques for seismic applications," U.S. patent 6,834,236 (December 21, 2004).
- Le Crom, B., and Castaigns, M. (2010). "Shear horizontal guided wave modes to infer the shear stiffness of adhesive bond layers," *J. Acoust. Soc. Am.* **127**(4), 2220–2230.
- Minonzio, J.-G., Talmant, M., and Laugier, P. (2010). "Guided wave phase velocity measurement using multi-emitter and multi-receiver arrays in the axial transmission configuration," *J. Acoust. Soc. Am.* **127**(5), 2913–2919.
- Prada, C., and Thomas, J.-L. (2003). "Experimental subwavelength localization of scatterers by decomposition of the time reversal operator interpreted as a covariance matrix," *J. Acoust. Soc. Am.* **114**(1), 235–243.

- Schmidt, R. O. (1986). "Multiple emitter location and signal parameter estimation," IEEE Trans. Antennas Propagat. **34**(3), 276–280.
- Williams, D. B., and Madisetti, V. K. (1999). "Detection: Determining the number of sources," in *Digital Signal Processing Handbook* (CRC Press, Boca Raton, FL).
- Xu, K., Minonzio, J.-G., Ta, D., Hu, B., Wang, W., and Laugier, P. (2016). "Sparse SVD method for high-resolution extraction of the dispersion curves of ultrasonic guided waves," IEEE Trans. Ultrasonics, Ferroelectr., Frequency Control **63**(10), 1514–1524.
- Zhao, W., Li, M., Harley, J. B., Jin, Y., Moura, J. M. F., and Zhu, J. (2017). "Reconstruction of Lamb wave dispersion curves by sparse representation with continuity constraints," J. Acoust. Soc. Am. **141**(2), 749–763.